



ELSEVIER

Contents lists available at SciVerse ScienceDirect

## Earth and Planetary Science Letters

journal homepage: [www.elsevier.com/locate/epsl](http://www.elsevier.com/locate/epsl)

## Organization of the tectonic plates in the last 200 Myr

Gabriele Morra<sup>a,\*</sup>, Maria Seton<sup>b</sup>, Leonardo Quevedo<sup>b</sup>, R. Dietmar Müller<sup>b</sup><sup>a</sup> Marine Geosciences and Geodynamics Group, School of Earth and Environmental Sciences, Seoul National University, Seoul 151-742, South Korea<sup>b</sup> Earthbyte Group, School of Geosciences, University of Sydney, Australia

## ARTICLE INFO

## Article history:

Received 13 February 2013

Received in revised form

12 April 2013

Accepted 14 April 2013

Editor: Y. Ricard

## Keywords:

plate reconstructions

global geodynamics

plate size

top–down tectonics

mantle convection

bottom–up tectonics

## ABSTRACT

The present tessellation of the Earth's surface into tectonic plates displays a remarkably regular plate size distribution, described by either one (Sornette and Pisarenko, 2003) or two (Bird, 2003) statistically distinct groups, characterised by large and small plate size. A unique distribution implies a hierarchical structure from the largest to the smallest plate. Alternatively, two distributions indicate distinct evolutionary laws for large and small plates, the first tied to mantle flow, the second determined by a hierarchical fragmentation process. We analyse detailed reconstructions of plate boundaries during the last 200 Myr and find that (i) large and small plates display distinct statistical distributions, (ii) the small plates display little organisational change since 60 Ma and (iii) the large plates oscillate between heterogeneous (200–170 Myr and 65–50 Ma) and homogeneous (120–100 Ma) plate tessellations on a timescale of about 100 Myr. Heterogeneous states are reached more rapidly, while the plate configuration decays into homogeneous states following a slower asymptotic curve, suggesting that heterogeneous configurations are excited states while homogeneous tessellations are equilibrium states. We explain this evolution by proposing a model that alternates between bottom- and top-driven Earth dynamics, physically described by fluid-dynamic analogies, the Rayleigh–Benard and Bénard–Marangoni convection, respectively. We discuss the implications for true polar wander (TPW), global kinematic reorganisations (50 and 100 Ma) and the Earth's magnetic field inversion frequency.

© 2013 Elsevier B.V. All rights reserved.

## 1. Introduction

Plate tectonic cycles occur at several timescales, with seismic cycles on the order of hundreds to thousands years, and tectonic cycles of several hundreds of million years for the formation and break-up of supercontinents (Wilson cycle) such as Pangea and Rodinia. Regional plate tectonics is driven by subduction, in which slabs require 5–15 Myr to reach the boundary between the Earth's upper and lower mantle; a time period also required to open back-arc basins (Faccenna et al., 1996; Fukao et al., 2009; Stegman et al., 2010). The intermediate timescale between tens and hundreds of million years is not yet well understood. In this timeframe, apparent polar wander studies and plate reconstructions have identified plate reorganisations at intervals of about 50 Myr (Torsvik et al., 2008a), and sea-level studies have identified cycles at the timescale of 10–100 Myr (Miall, 1990). Yet the geodynamic origin of these observations is still unclear. Here we use a statistical analysis of the tessellation of rigid plates of the Earth's surface in the past to explore the dynamics governing this timescale.

The Pacific plate is the largest tectonic plate on Earth and its boundaries host the majority of subduction zones and earthquakes. The second largest plate, Africa, is at the antipode of the Pacific and is mostly surrounded by mid-ocean ridges. Each of them is located above one of the two low velocity zones at the bottom of the lower mantle, usually associated with a superswell caused by thermal anomaly (Schuberth et al., 2009) or compositional differentiation (van der Hilst and Kárason, 1999). Such a bimodal configuration is illustrated by the Earth's plate tessellation in Fig. 1, based on the dataset in Gurnis et al. (2012), where the grey intensity is proportional to plate size. Combined with another six major plates (Eurasia, Australia, Antarctica, North and South America, and Nazca) these eight large plates cover most of the surface of the Earth. Whether this configuration is coincidental, due to inter-plate stresses or an outcome of the Earth dynamics is topic of research (Anderson, 2002; Grigné et al., 2007; Lowman, 2011; O'Neill et al., 2008, 2009, Zhong et al., 2007).

The remaining plates are one or more orders of magnitude smaller and their size follows a statistical distribution (Pareto Law) which may reflect some sort of fragmentation mechanism (Bird, 2003; Sornette and Pisarenko, 2003). Complex processes such as fragmentation are often revealed by geometrical self-similarity, where a recurring pattern occurs over a wide range of scales. Such a multiscale property is conventionally described by a power-law, a function of the form  $S(x) \propto x^{-1/\alpha} = x^{-\beta}$  where  $S$  is the observable at

\* Corresponding author.

E-mail address: [gabrielemorra@gmail.com](mailto:gabrielemorra@gmail.com) (G. Morra).

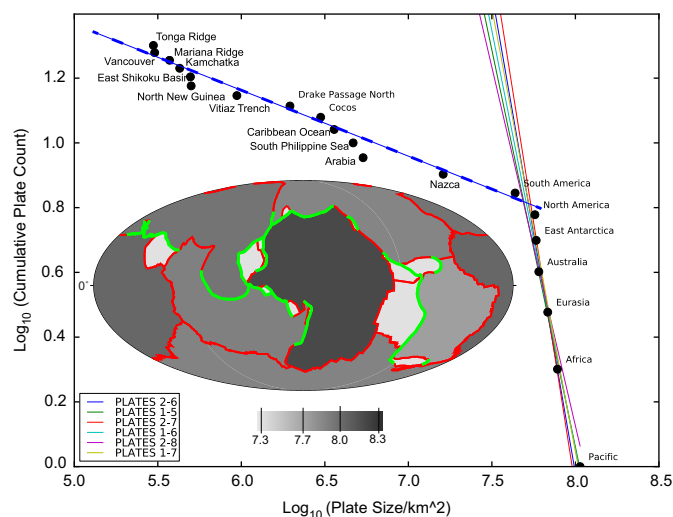


**Fig. 1.** The planetary map represents the Earth's present tessellation. Grey scale intensity is proportional to the logarithm of plate size. Green boundary lines indicate convergent margins while red lines show the location of spreading boundaries. The map illustrates the polarity of the tectonic system in which the two greatest plates, the African and Pacific, are at the antipodes of one another. The plot represents the logarithm of complementary "cumulative plate count" (Y-axis) vs. the logarithm of the plate size (X-axis) of the 22 plates shown in the global map (data from Gurnis et al. (2012)). The coloured lines are based on 5 fits of overlapping subsets of plates. Two regimes are identifiable: (i) below  $\log(\text{Size})=7.5$  the small plates follow a power-law with an exponent  $\alpha \sim 3-5$ , (ii) the largest 6-7 plates follow a steeper slope with  $\alpha=0.3$ . (For interpretation of the references to colour in this figure legend, the reader is referred to the web version of this article.)

the scale  $x$  and the exponent  $\alpha$  (and its inverse  $\beta$ ) is a scale-independent coefficient. The simplest way to determine  $\alpha$  is by quantifying the slope of the straight line that characterises its log-log representation. Bird (2003) analysed the relationship between *plate area*  $A$  and *cumulative plate count*  $N(A)$  (the number of plates with area greater than  $A$ ) for his highly refined database composed of 42 plates, obtaining the best fit  $N(A) \propto A^{-1/\alpha} = A^{-\beta}$  with  $\alpha \sim 4$  ( $\beta \sim 0.25$ ). In Fig. 1 we perform the same analysis on a different dataset of reconstructed plate boundaries in the past 140 Myr (Gurnis et al., 2012) and obtain a very similar result for the small plates at present time ( $\beta_{sp} = 0.22$ ). An even more detailed dataset has been put forward for the last 200 Myr (Seton et al., 2012), showing the same result. We will refer to this most recent dataset in the rest of the paper (Fig. 2).

It has been debated whether the distribution of the largest plates may reflect the same process proposed for the smaller ones (e.g. Bird, 2003; Fig. 19). If they follow a different distribution, this must reflect the complex interaction between surface plate motion and mantle convection. Fig. 1 already suggests that the large plates form a distinct statistical group; however such a small number of data points do not provide sufficient evidence. In effect it has been shown by Sornette and Pisarenko (2003) that a modified Pareto Law, corrected for the finite size of the Earth, would absorb the observed "kink" between the two distributions. In this work we resolve this controversy by analysing the tessellation formed by plate boundaries in the past 200 Myr, showing that the kink is a permanent feature in time, therefore not due to a fluctuation in the statistics as suggested by Sornette and Pisarenko (2003). We employ this result to obtain new insights on the evolution of the Earth's mantle and global tectonics.

## 2. Analysis of the tectonic reconstructions

Kinematic reconstructions are built upon a wealth of unrelated geological and geophysical data, making a precise quantification of

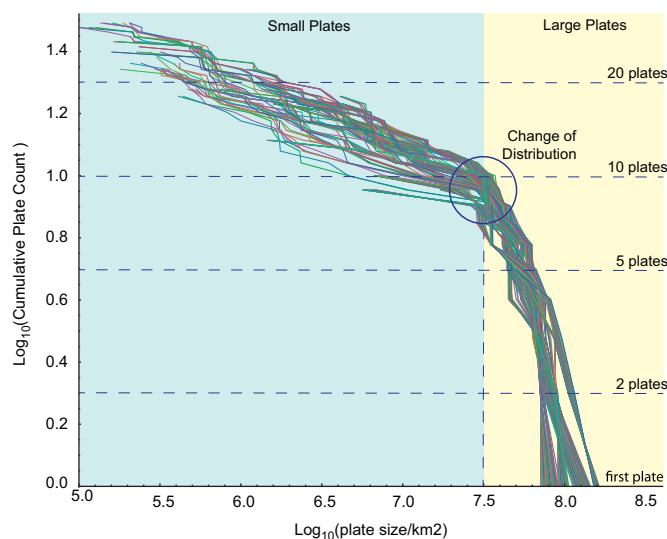


**Fig. 2.** Plot of the logarithm of the plate size vs. logarithm of complementary "cumulative plate count", as in Fig. 1, for each reconstructed plate tessellation in the past 200 Myr. The number of reconstructed plates (Seton et al., 2012) decreases towards the past from 31 at Present time down to only 10 at 200 Ma (detailed plot in the Supplementary material). The distinction between the large and small plates distributions is observed at any time. The critical plate size at which the distribution changes is about  $10^{7.5}$  km<sup>2</sup>, slightly less than the square of the Earth radius ( $6371 \text{ km}$ )<sup>2</sup> and Cumulative Plate Count equal to 8..

the uncertainties extremely difficult. Stronger constraints exist for the past 100 million of years, for which the finite rotations of the plates are reconstructed using ocean-floor magnetic lineations. A recent estimation of the errors involved in the identification of the timing associated to each isochrone finds no more than few million years (Iaffaldano et al., 2012). The uncertainty associated with the physical location of plate boundaries is greater and reaches one hundred of kilometres (e.g. by multiplying the time uncertainties by the fastest plate velocities:  $1 \text{ Myr} \times 10 \text{ cm/yr} = 100 \text{ km}$ ). Completely vanished basins cannot be directly identified, but plate boundary inception and cessation can be traced at subduction zones, allowing further constraints on the ancient geometry of the reconstructed plates.

Another source of uncertainty is the true-polar wander (TPW) correction. Before 100 Ma we adopted a TPW correction based on paleomagnetic models (Torsvik et al., 2008a). More details have been published in methodological and review papers (Gurnis et al., 2012; Seton et al., 2012). Although a complete estimation of the errors associated with the reconstruction is not yet possible, we have taken the maximum care in testing the effect of different reconstructions presenting here only the most robust results. We do not interpret the statistics of the small plates earlier than 60 Ma because the number of small plates is too small. For the large plates we analyse only the main statistical features (mean and standard deviation). Any bias in the plate size data is excluded because the boundary model used in this work has been developed totally independently.

### 2.1. One or two plate size distributions

Fig. 2 shows the relationship between *plate area*  $A$  and *cumulative plate count*  $N(A)$ , as in Fig. 1 for present time, at every million years for the past 200 Myr based on the most recent tectonic reconstruction (Seton et al., 2012). Despite the noise in the data and the uncertainties in the oldest reconstructions, the distribution remains remarkably stable for the past 200 Myr. Furthermore the distinction between large and small plates is always present, at about  $\log_{10}(N(A)) = 0.9$ , which corresponds to

$N=8$  and to  $A=10^{7.5}$  km<sup>2</sup>. Based on this result, in the rest of the paper we will always define large plates (LP) among the first 8, and small plates (SP) among the ones with cumulative number above or equal to 9.

We have tested the hypothesis that small and large plates form one or two distributions, benchmarking how well the reconstructions are fit by a Pareto Law modified by the constrain of the Earth's finite size. We implemented the algorithm explained in Sornette and Pisarenko (2003) in Mathematica and plot the distribution vs. reconstructed data and tested with our different dataset. Sornette and Pisarenko (2003) use the Maximum Likelihood method to analyse the 42 plates model of Bird (2003) and observe that the kink at present time is compatible with a corridor around the median at the 95% confidence level, implying that the kink could be a “fluctuation” at present time and the plates be part of the same statistical distribution. With our different and larger dataset, composed by less plates but with a much greater wealth of data given by their evolution in time, we find that the “kink” in Fig. 2 is distant between 2 and 3 times the standard deviation from the median of the distribution predicted by the constrained Pareto Law and it persists during the past 200 Ma. This result excludes the possibility that the separation between large and small plates in the present distribution might be a fluctuation. We therefore conclude that, despite the uncertainties in the tectonic reconstructions small and large plates follow separate statistics, due to distinct causes. It is therefore worth to separately analyse their distributions and investigate the implications for global geodynamics (algorithms and detailed plots in the Supplementary material).

We have determined the slope  $\alpha_{SP}$  associated with the size of the small plates back to 60 Ma with a standard deviation less than 10% (details further in the text). We find that the distribution has not substantially changed during the Cenozoic, while the data do not allow a definitive estimation for older times. The statistical properties of the large plates, instead, have been calculated back to

200 Ma. At least 8 plates have been reconstructed at any time in the past, with the exception of the time earlier than the break-up of Pangea (about 180 Ma).

## 2.2. Small plates

The calculation of  $\alpha_{SP}$  (inverse of  $\beta_{SP}$ ), the exponent associated to small plates, requires a minimum number of plates to be statistically significant. The total number of reconstructed plates during the Cenozoic oscillates between 18 and 31 (detailed plot in the Supplementary Material). In order to evaluate  $\alpha_{SP}$  on the largest possible set, we excluded the largest 8 plates from the SP set and we minimised the risk of down-sampling (Bird, 2003) through averaging only the 10 largest among the SP. We have therefore estimated  $\alpha_{SP}$  with a linear regression fit on six subsets composed by the plate indexes 9–18, 9–19, 9–20, 10–19, 10–20, 10–21 (Fig. 3).

As shown in Fig. 2, the 10–12 plates of each SP sample corresponds to more than one order of magnitude in terms of plate size. We did not calculate  $\alpha_{SP}$  earlier than 60 Ma as the challenge of reliably reconstructing the small basins becomes prohibitive at older times and the record of the small plates becomes almost inexistent before 140 Ma. We also calculated the residuals from the estimation of  $\alpha_{SP}$   $R_{es} = \text{Sqrt}\{\sum[\log_{10}[N(A_i)] - (\log_{10}[i] \times \alpha_{SP})]^2\}/(n-1)$  and find that  $R_{es}$  is always within the range  $[1 \times 10^{-1} - 3 \times 10^{-1}]$ , one order of magnitude smaller of the range of variation of  $\log_{10}[N(A_i)]$ , which is  $[0.9-1.3]$  (more in the Supplementary material).

Most of the small plates exist for less than 10–20 Myr. This implies that 50 Myr is a sufficiently long time for observing the steadiness of  $\alpha_{SP}$  through time. The resulting estimate of  $\alpha_{SP}$  (Fig. 3) is in the interval  $\alpha_{SP}=[3-5]$ , or  $\beta_{SP}=[0.2-0.33]$ . The best fit is graphically represented every 10 Myr in Fig. 5A.  $\beta_{SP}$  remains always close to the value ( $\beta=0.25$ ) calculated at present time (Bird, 2003). This confirms the compatibility of this statistics with the

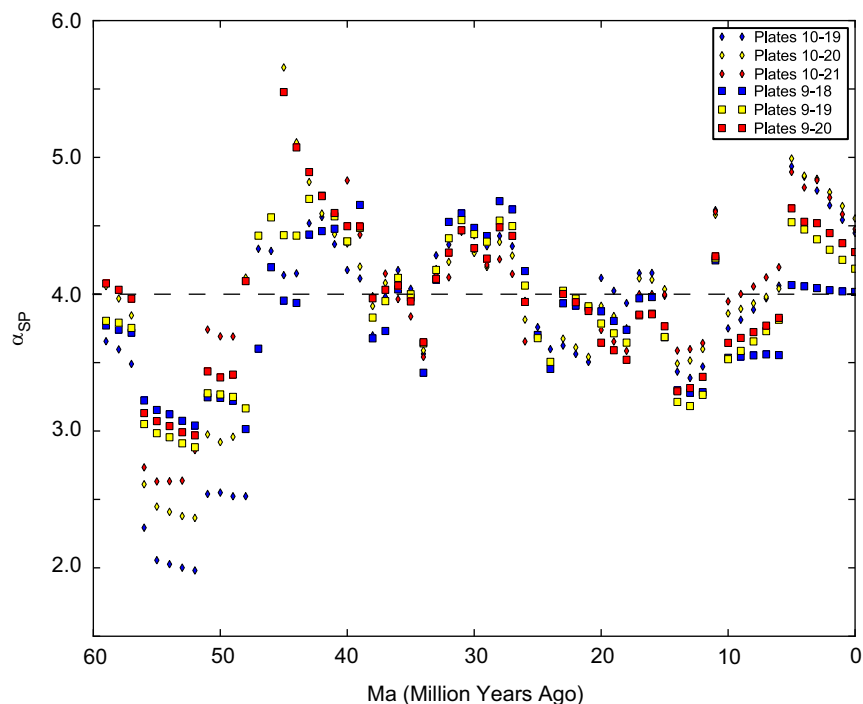


**Fig. 3.** Time evolution of the best fitting parameter  $\alpha_{SP}$  (small plates) at each million year in the past since 60 Ma. No clear pattern appears, besides small oscillations between 3 and 5, around the value of 4. The value of 4 coincides with the prediction from classical fragmentation model ( $\beta=1/\alpha-1/4=0.25$ ). The fluctuations from  $\alpha=4$  are larger at older times, possibly due to the increase of uncertainties of plate boundary location and reduced number of reconstructed small plates. The deviation of the data from the curve is shown in the Supplementary Materials.

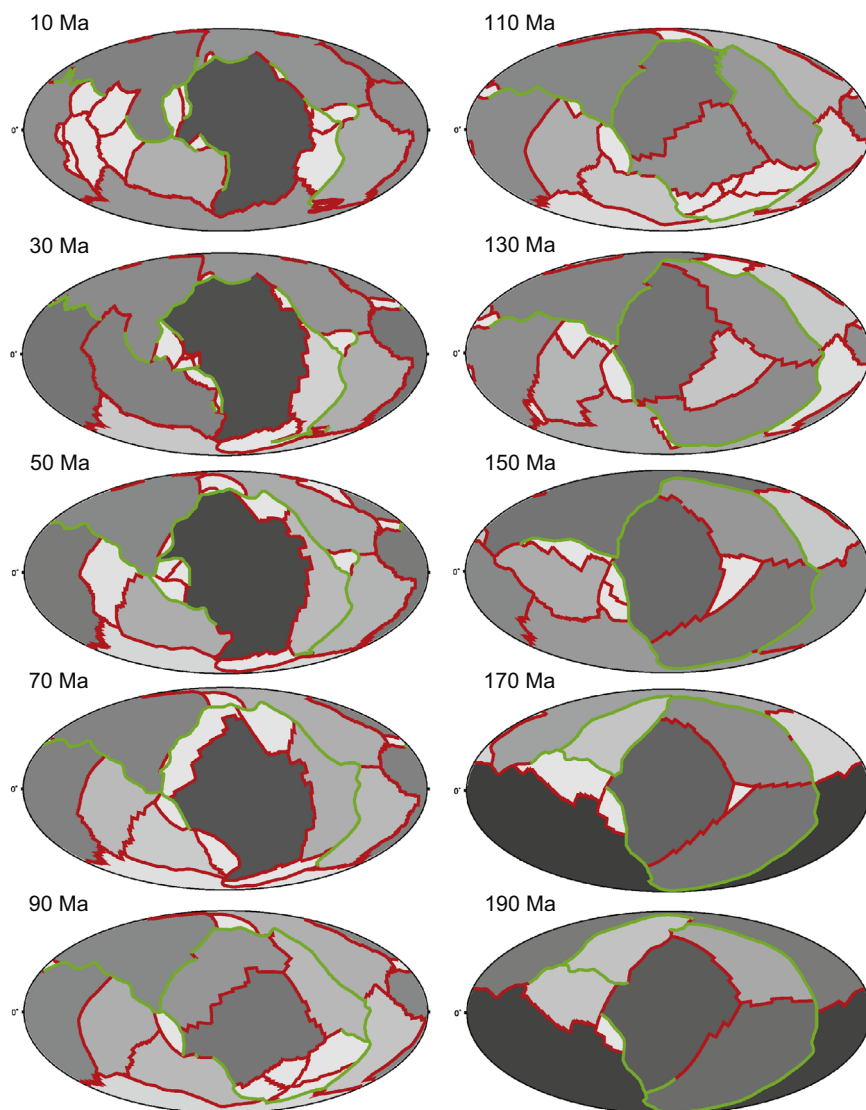


**Fig. 4.** Earth Surface tessellation for the last 190 Myr: darker grey indicates larger plate size (legend in Fig. 1). Strongly heterogeneous tessellations have a large-dark Pacific (or Izanagi) Plate surrounded by smaller grey plates (e.g. 50 Ma). Homogeneous tessellations are uniformly grey (e.g. 110 Ma). Green boundary lines represent convergent margins while red lines indicate spreading plate boundaries. (For interpretation of the references to colour in this figure legend, the reader is referred to the web version of this article.)

analogy with a fragmentation model and other complex systems such as joint spacing (Sornette and Pisarenko, 2003).

### 2.3. Large plates

The propagation of errors in plate boundary reconstructions back in time has a minor effect on the large plates compared to the small ones. In Fig. 4 we display the Earth Surface tessellation every 10 Myr for the last 200 Myr where, as in Fig. 1, darker grey indicates larger plate size, green lines represent convergent margins and red lines refer to divergent boundaries. In Fig. 5B we plot the linear best fit for the large plates considering the five subsets indicated by the plate index: 1–5, 1–6, 1–7, 2–6, 2–7, where 1 is the largest plate. These subsets are chosen to be always part of the large plates ( $N < 8$ ). We find that  $\alpha_{LP}$  is always above 1, reaching an almost infinite value when the large plates have similar size. These tessellations are the most *homogeneous*, while the ones for which  $\alpha_{LP}$  is minimum they are strongly *heterogeneous*, as the large plate sizes vary mostly. Very heterogeneous tessellations are reached at ~60 Ma, while homogeneous tessellations ~110 Ma.

The statistical uncertainty associated to the calculation of  $\alpha_{LP}$  and  $\beta_{LP}$  can be large due to the small size of the sample, therefore we analyse only the “mean”  $\mu_{LP}$  and “standard deviation”  $\sigma_{LP}$  that are always well defined for a non-singular distribution. We define  $\sigma_{LP}$  as  $\text{Sqrt}\{\sum[A_i - \mu_{LP}]^2 / (n-1)\}$ , where  $\mu_{LP} = \sum A_i / n$ ,  $n$  is the sample size and  $A_i$  is each plate area. Minimum values of  $\sigma_{LP}$  indicate homogeneous tessellation, while maximum heterogeneous configurations. The time evolution of  $\sigma_{LP}$  is shown in Fig. 6 for the largest 6, 7 and 8 plates, displaying a pattern largely independent on the size of the subset. The jumps in the values of  $\sigma_{LP}$  are associated with major global tectonic events, such as when a ridge begins or stops to spread. Labels on the figure indicate the most important ones.

### 3. Evolution of the Earth's tessellation and major tectonic events

Our analysis of the reconstructed plate boundaries in the past 200 Myr shows that the distinction between large and small plates statistics is a characteristic of plate tectonics on Earth,

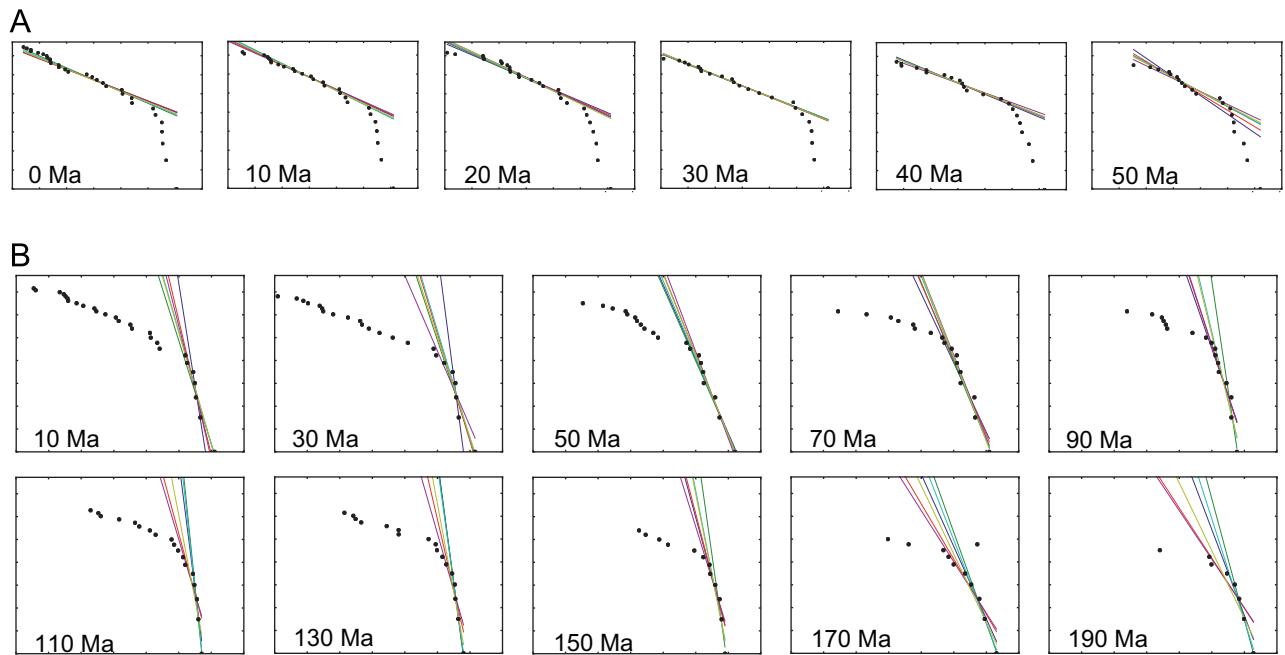


**Fig. 5.** (A) Fits of the log-log statistical ordered representation of the small plate sizes in the past 50 Ma. (B) The same as in A but for the large plates since 200 Ma. Lowest values (~110 Ma) correspond to maps with uniform plate tessellation, while maximum (~60 Ma) correspond to heterogeneous tessellations.

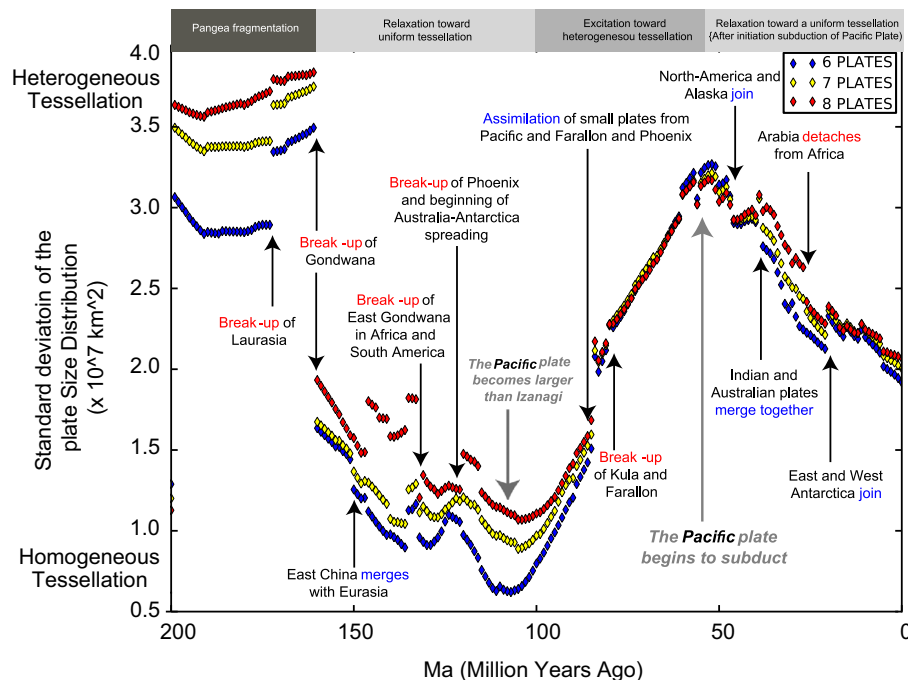


**Fig. 6.** Time evolution of the “standard deviation”  $\sigma_{LP}$  of the plate size every one million years, for the largest 6, 7 and 8 plates. Minimum and maximum are in correspondence with the main reorganisations (indicated in grey). The main geological events in the last 200 Ma triggering large variations of  $\sigma_{LP}$  are indicated either in red (plate splitting) or in blue (plate merging). (For interpretation of the references to colour in this figure legend, the reader is referred to the web version of this article.)

as it emerges from the resilience of the “kink” that divides the two distributions. Focusing on large plates, covering the major portion of the Earth surface, the time evolution of  $\sigma_{LP}$  (Fig. 6) suggests the existence of an alternation of homogeneous and heterogeneous tessellations, at a time scale around 100 Myr. Homogeneous tessellations are clearly visible in Fig. 4, corresponding to the minimum of  $\sigma_{LP}$  (110 Ma), in which the plate colours are uniformly grey, indicating virtually no difference in large plate sizes. Conversely when  $\sigma_{LP}$  reaches its maximum value (~60 Ma) the plate

colouring shows great differentiation, indicating that the tessellation has reached a maximum degree of heterogeneity.

The evolution of  $\sigma_{LP}$  is also deeply linked to global plate reorganisations, as it emerges analysing in detail the two turning points (~120–100 Ma and ~65–50 Ma) of the evolution of  $\sigma_{LP}$  after the break-up of Pangea, Laurasia and Gondwana (~170 Ma). In fact the two main plate reorganisations in the last 200 Myr (at ~100 Ma and ~50 Ma) (Matthews et al., 2012; Wessel et al., 2006) have been global as they involved the Pacific and other large

plates. The reorganisation at ~50 Ma, visible in bends of Pacific hotspot tracks (Veevers, 2000), is likely due to the subduction of the ridge between the Izanagi and Pacific plates (Goes et al., 2008; Whittaker et al., 2007), therefore it marks the beginning of subduction of the Pacific Plate. This event, reducing the size of the Pacific basin and leaving space for the other large plates to grow, causes the decrease of plate heterogeneity, and therefore of  $\sigma_{LP}$ . This shows one mechanism linking major tectonic events and evolution of  $\sigma_{LP}$ .

The other turning point of  $\sigma_{LP}$  is its minimum that corresponds to the other main plate kinematic reorganisation originally dated between 120 and 80 Ma (Veevers, 2000), and more recently constrained between 105 and 100 Ma (Matthews et al., 2012). Evidence of this event are in the bends observed in several hot spot tracks in the western Pacific (Wessel et al., 2006) and in fracture zones in the eastern Indian ocean. The causes of this major change are still debated, potentially being Top-Down, such as the termination of the eastern Gondwanaland subduction or Bottom-Up, such as plume-ridge interactions (Matthews et al., 2012). Regardless on the mechanism, we observe that the growth of  $\sigma_{LP}$  coincides with the replacement of the largest plate of the global tessellation before 100 Ma (the Izanagi Plate) with the Pacific Plate, which inverts the trend from slow relaxation towards homogeneous tessellation since the break-up of Laurasia and Gondwana (200–160 Ma). After reaching the peak of tessellation heterogeneity at 60–50 Ma, the system slowly returns towards homogenisation, which still continues.

#### 4. Driving mechanisms

Many works have focused on the interplay between surface tectonics and mantle convection finding that the lithospheric strength controls the onset and stability of plate tectonics (Bercovici, 1998; Tackley, 2000; Trompert and Hansen, 1998), self organising as a top-down, subduction driven, process (Buffett et al., 1994; Christensen, 2001; Christensen and Yuen, 1984; Forsyth and Uyeda, 1975; King, 2001; Lithgow-Bertelloni and Richards, 1998), although uncertainties remain on the quantification of plate stresses (Becker and O'Connell, 2001; Conrad and Lithgow-Bertelloni, 2002; Lithgow-Bertelloni and Gynn, 2004; Wuming et al., 1992), the initiation of new divergent plate boundaries (Allken et al., 2011; Gerya, 2010; Regenauer-Lieb et al., 2006), the force transmission at convergent margins (Becker et al., 1999; Buffett and Heuret, 2011; Capitanio et al., 2009b; Conrad and Hager, 1999; Husson et al., 2012; Iaffaldano et al., 2006; Zhong and Gurnis, 1995) and the fate of the slab in the lower mantle (Lee and King, 2011; Morra et al., 2012, 2010; Ribe, 2010; Li and Ribe, 2012). These works converge towards a “top-down” view of plate tectonics, in which the driving force is the sinking of heavy and stiff slabs and in which the stress is propagated to the surface through the pull of the lithosphere at subduction zones. The timescale associated to this dynamics is of tens of million years, as inferred from reconstructing plate motions from lower mantle slab remnants (van der Meer et al., 2009).

The longer timescales, of hundreds of million years, is associated to the convection of the entire mantle (Lowman, 2011; Ricard and Vigny, 1989; van der Meer et al., 2009), and has been intensively investigated modelling the active role of thermal circulation (Cramer et al., 2012; O'Farrell et al., 2013; van der Meer et al., 2009; Zhong et al., 2000), the insulation of continents (Coltice et al., 2012; Grigné et al., 2007; Phillips and Coltice, 2010), compositional differentiation of the lower mantle, in particular below the African and Pacific plates (Brandenburg and van Keken, 2007; Deschamps et al., 2012; Torsvik et al., 2008b; van Keken and Ballentine, 1998), the long term evolution of the plate morphology

(Lowman et al., 2001; Monnereau and Quéré, 2001; Stein et al., 2012) and the link between the entire mantle flow and plate motions (Conrad and Behn, 2010; Husson, 2012; King et al., 2002; Lowman et al., 2003). Furthermore a recent set of studies has focused on the relationship between degree two mantle convection (Rolf et al., 2012) and the observed seismic anomalies in the lower mantle (Dziewonski et al., 2010), supercontinent cycles (Zhong et al., 2007) and true polar wander (Creveling et al., 2012; Steinberger and Torsvik, 2010) suggesting that at a timescale above 100 Myr they are interrelated. The long-term perspective associated with these works advocates for a “bottom-up” interpretation of the interplay between mantle-flow and plate tectonics.

Bottom-up and top-down paradigms of plate tectonics have distinct fluid-dynamic analogies. Rayleigh-Bénard, or Bénard, convection is defined by the overturning of a heated fluid (either from the bottom or from within), is analogous of bottom-up mantle convection (Bercovici et al., 2000; Yanagisawa and Yamagishi, 2005) and is characterised by homogeneous cell sizes (Yoshida, 2010; Zhang et al., 2009; Zhong et al., 2008). This analogy, although unable to capture compositional complexities and viscosity variations, allows estimating the vigour of Bénard convection from the Rayleigh number defined as  $Ra = g\alpha\rho\Delta Td^3/\nu\kappa$  where  $d$  and  $\Delta T$  are the size and the temperature variation of the system,  $\rho$  the density,  $\alpha$  the thermal expansion,  $\nu$  the dynamic viscosity and  $\kappa$  the thermal diffusivity. Bénard-Marangoni, or simply Marangoni, convection (Scriven and Sterling, 1964; Thess et al., 1997) has been instead proposed as an analogue of top-down plate tectonics (Anderson, 2001; Lemery et al., 2000; Ricard, 2007), due to the analogy between the viscoelastic properties of the stiff lithospheric core (Hirth and Kohlstedt, 1996; Regenauer-Lieb et al., 2006) and surface tension. Marangoni convection is not a perfect analogy as it is driven by the lateral gradient of stress, while on Earth the stiffness of the plate core has a different role, allowing the transmission of the pull of the subducting slab to the surface plates (Capitanio et al., 2009a) and increasing the stiffness of the plates (Bercovici et al., 2000). Still this analogy is useful as it allows quantifying the importance of the plate strength to the mantle convection dynamics, through the Marangoni number  $Mo = -\gamma\Delta Td/\nu\kappa$ , where  $\gamma = df/dT$  is the analogue of the derivative of surface tension  $df$  per temperature variation  $dT$  (Lemery et al., 2000; Ricard, 2007). The importance of lithospheric stiffness is confirmed by numerical models that have shown how the aspect ratio of the convection cells changes in function of plate strength (Gurnis, 1988; Moresi et al., 2002; Morra et al., 2012; Zhong et al., 2007).

When  $Ra$  is above ~1000 the thermal gradient is sufficient to initiate bottom-up convection, while when  $Mo$  is over ~100 top-down Marangoni-like convection can initiate. It is known that  $Ra$  for the Earth's mantle is well above 1000, while  $Mo$  is less investigated. To quantify  $Mo$  one needs to define an analogue of surface tension,  $\gamma$  that we determined from the stiffness of the lithospheric core. This 10–30 km thick layer of the oceanic plate controls plate strength (Capitanio et al., 2007; Regenauer-Lieb et al., 2006; Watts and Zhong, 2000), the radius of curvature of the slab during subduction (Buffett and Rowley, 2006; Capitanio et al., 2009b), and the predisposition of the plate to fragmentation (Regenauer-Lieb et al., 2001). Based on this knowledge,  $\gamma$  for the Earth is determined by the ratio between the plate stresses (ridge push and the slab pull,  $\sigma \sim [1 \times 10^{12} - 5 \times 10^{13}]$  Pa m) and the temperature variation in the lithosphere ( $\Delta T \sim [500 - 1000]$  K), which results in the range  $\gamma = [1 \times 10^9 - 1 \times 10^{11}]$  Pa m/K.  $Mo$  can be straightforwardly calculated assuming  $\gamma\Delta T = \sigma$ ,  $\nu = 10^{21} - 10^{22}$  Pa s and  $\kappa = 10^{-5}$  m<sup>2</sup>/s, implying  $Mo = \sigma d/\nu\kappa \approx [10 - 10^4]$ , around and above the critical value  $Mo_c \sim 100$ , where the high value  $10^4$  is for a stiff old lithosphere (high  $\sigma$ ) subducting in the upper mantle (low  $\nu$ ).

This simple calculation shows how the Marangoni number can nail to the importance of the plate strength in plate tectonics, as also demonstrated by many numerical models (Moresi et al., 2002; Zhong et al., 2007).

The two driving mechanisms can be compared analysing the ratio  $Ra/Mo$  e.g. (Skarda and McCaughan, 1994), equal to  $g\alpha\rho d^2/\gamma$ , assumed the same thickness and viscosity for the two convective mechanisms. This approach allows eliminating the viscosity and thermal diffusivity, which are highly uncertain for the mantle, and the ambiguous thermal variation in the lithosphere. The critical ratio is  $Ra/Mo \approx 10$ : if  $Ra/Mo \gg 10$ , buoyancy dominates (Bénard convection); if  $Ra/Mo \ll 10$ , the stiff elastic stresses in the lithosphere will impose the Marangoni convection regime. When the system is dominated by Bénard convection it will tend to symmetric, homogeneous tessellations, while Marangoni domination will induce heterogeneously sized convection cells. Assuming a thermal expansion ( $\alpha \sim 4 \times 10^{-5} K^{-1}$ ), density ( $\rho \sim 3000 \text{ Kg/m}^3$ ) and thickness of the convective domain ( $d = 600\text{--}2800 \text{ km}$ ) and putting everything together, the resulting range for  $Ra/Mo$  is  $[5\text{--}10^4]$ , close and above the critical value ( $Ra/Mo \sim 10$ ). This ratio results even lower if we assume that the Marangoni mechanism is controlled by the upper mantle viscosity ( $Mo \sim 1/\nu_{UM}$ ), while Bénard by the lower mantle one ( $Ra \sim 1/\nu_{LM}$ ), obtaining  $Ra/Mo \sim (\nu_{UM}/\nu_{LM}) \sim 10^{-1}$ , i.e.  $Ra/Mo$  in the range  $[0.5\text{--}10^4]$ . We propose here that the observed evolution of  $\sigma_{LP}$ , characterising the alternation of homogeneous and heterogeneous tessellations, is in fact the surface expression of an alternating dominance of either top-down (Marangoni) or bottom-up (Bénard) driving mechanisms.

Low values of  $Ra/Mo$  are reached for old stiffer plates (maximum  $\gamma$ ) interacting with the upper mantle (minimum  $d$ ). If one instead calculates  $Ra/Mo$  only for the entire mantle ( $d = 2800 \text{ km}$ ) one systematically obtains values of the order of  $10^2\text{--}10^4$ , indicating that the interaction of a stiff lithosphere with a weak upper mantle is a key factor for the induction of the top-down mode. This is in agreement with numerical models of plate tectonics and mantle convection on a sphere (Zhong et al., 2007). The high values of  $Ra/Mo$  when  $d = 2800 \text{ km}$  suggest that a bottom-up driving mantle will slowly push the system towards a Bénard state, i.e. homogeneous tessellations. Instead the top-down dynamic regime will pull away the system from equilibrium towards Marangoni states, i.e. heterogeneous configurations. Therefore the alternation between bottom-up and top-down convection modes is an expected feature of plate tectonics for the specific Earth layered radial viscosity structure and of the stiff lithosphere, but the Bénard convection is always present while the Marangoni one is episodic and controlled by the largest subducting plates.

Following this interpretation the growth of  $\sigma_{LP}$  at 100 Ma is due to a departure from a “Bénard” equilibrium state towards a “Marangoni” convection style, in which the stiffness of the oceanic plates, Izanagi first, the Pacific later, has perturbed the system from its homogeneous tessellation. This view, besides explaining key observations, reconciles the debate between top and bottom driven plate tectonics, suggesting that in the timescale of 100 Myr and above the Earth system tends to be dominated by the Bénard-style mode-2 convection, while the presence of very large and oceanic plates, such as the Pacific, perturbs the system through a Marangoni mechanism and pushes it away from an homogeneous equilibrium state.

## 5. Other implications

There are other potential implications in relationship with the True Polar Wander (TPW), the motion of the Earth's axis position. It has been already observed that there exists a correlation

between geoid, position of slab subduction and superswells (Richards and Engebretson, 1992; Zhong et al., 2007). Furthermore the analysis of the TPW during the past 300 Myr has revealed periods of time of the order of hundred million years characterised by a relatively fast Polar Wander of up to 1 deg/Myr for 10–30 Myr (e.g. before 100 Ma), and periods of relative TPW quiescence such as the last 100 Myr (Steinberger and Torsvik, 2008). Although our analysis of plate sizes does not allow pointing to the exact mechanism causing these fluctuations, it nevertheless suggests that at 100 Ma the style of global dynamics has changed from top-down to bottom-up tectonics. Before 100 Ma the periods of intense TPW resulted from greater continental mobilisation and larger number break-up events (Fig. 6). Conversely the TPW quiescence in the last 100 Myr coincided with less break-up and more merging events and, in the last 60 Myr, in a relaxation of the surface tessellation. These correspondences corroborate the hypothesis that the variations of global plate tessellation and TPW must be related.

It has been proposed that the frequency of geodynamo reversals at the timescale of tens of millions of years is related to core–mantle boundary heat flow at the equator, i.e. where the superswells are located (Olson et al., 2010). The Earth's spin axis, which in turn dictates the core fluid motion, tends to align with the maximum non-hydrostatic inertia axis. This implies that the changes of the surface tessellation that are related to the size and location of slabs and of the thermochemical piles, will modify the boundary conditions and therefore the inversion frequency. Geodynamo models suggest that the 120–80 Ma reversal quiescence, the Cretaceous Normal Superchron, has been caused by low heat-flow at the core–mantle boundary (Aubert et al., 2009). This time coincides with the minimum of  $\sigma_{LP}$ , i.e. maximum tessellation homogeneity, when, we propose, the flow was dominated by the Bénard-style mode-2 convection, causing a minimisation of heat flux below the super-swells (Zhong et al., 2007). If this hypothesis will be confirmed, it will allow also inferring the Earth's surface tessellation close to past episodes of reversal quiescence such as the Ordovician and Permo-Carboniferous Reversed Superchrons (Biggin et al., 2012).

## 6. Conclusions

We find that the evolution of the plate tessellation on the Earth in the past 200 Myr can be divided in two sets formed by small and large plates. The small plates, mostly generated by uncorrelated events, display a strikingly stable statistical pattern during the past 60 Myr, for which a sufficiently large set exists (Seton et al., 2012). The size of the small plates follows a power law distribution with exponent 0.25, which may indicate an underlying fragmentation model or other complex systems (Sornette and Pisarenko, 2003).

We find that other complex evolutionary laws, still largely unexplored by numerical models, govern the tessellation of Earth's largest plates. Our analysis demonstrates the existence of an alternation between homogeneous and heterogeneous configurations in the past 200 Myr. This may either indicate a new global tectonic cycle at the time scale of 100 Myr, superposed to the Wilson cycle, or episodic pulsations of the global tectonic system pushing the system away from “equilibrium” homogeneous tessellations towards “out of equilibrium” heterogeneous configurations, followed by the slow return to equilibrium. This alternation of heterogeneous and homogeneous tessellations relates apparently disconnected geologic events such as the assimilation of several small plates by the Pacific, Farallon and Phoenix plates; the splitting of the Kula from the Farallon Plate before 50 Ma; and the

Alaska–North America, East–West Antarctica and India–Australia plates merging during the relaxation phase of the last 50 Myr.

We propose that this evolution is caused by the interplay between top-down and bottom-up convection mechanisms, whose role is quantified by Marangoni and Rayleigh numbers, respectively. Our quantitative analysis illustrates how the specific radial viscosity layering of the Earth (strong lithosphere, weak upper mantle, stiffer lower mantle) produces the alternation of tessellations. In agreement with global numerical models (Zhong et al., 2007) (O'Neill et al., 2009) and mantle global tomography (Dziewonski et al., 2010), our analysis supports the hypothesis that the position of the two present largest plates (Pacific and Africa) at the antipodes and above the two largest deep mantle low-velocity zones naturally emerges from the dual nature of the global plate tectonic evolution. We also show that the variation from intense to quite TPW, and the related Cretaceous Normal Superchron, around 100 Ma is likely related to the simultaneous homogeneous tessellation caused by Bénard-style mode-2 convection.

Although our analysis of the largest reconstructed plates is robust and verified on two different dataset, it will need to be tested with improved reconstructions. Some conclusions presented here are speculative and alternative explanations could be proposed. The goal of this work is to indicate new directions of research for studying the interplay between mantle convection and plate tectonics.

#### Author contributions

G.M. designed the project, carried out the plate size analysis, developed the top-down (Marangoni) and bottom-up (Benard) analogies and made the figures; R.D.M. and M.S. developed the plate reconstructions; M.S. extracted plate boundaries and plate sizes; G.M. and R.D.M. elaborated the implications for global geodynamics.

#### Acknowledgements

G. Morra thanks the Swiss National Science Foundation for financial support (Advanced Researcher Fellowship PA0022-121475) and the support by the Korea government (MEST, 2009–0092790). L. Quevedo, M. Seton and D. Müller thank the Australian Research Council for financial support through DP0986377, DP0987713 and FL0992245, respectively. We thank G. Shephard, J. Whittaker, S. Williams for constructively criticising an early version of the manuscript.

#### Appendix A. Supplementary materials

Supplementary data associated with this article can be found in the online version at <http://dx.doi.org/10.1016/j.epsl.2013.04.020>.

#### References

- Allken, V., Huisman, R.S., Thieulot, C., 2011. Three-dimensional numerical modeling of upper crustal extensional systems. *J. Geophys. Res.* 116, B10409.
- Anderson, D.L., 2001. Top-down tectonics? *Science* 293, 2016–2018.
- Anderson, D.L., 2002. How many plates? *Geology* 30, 411–414.
- Aubert, J., Labrosse, S., Poitou, C., 2009. Modelling the palaeo-evolution of the geodynamo. *Geophys. J. Int.* 179, 1414–1428.
- Becker, T.W., Faccenna, C., O'Connell, R.J., Giardini, D., 1999. The development of slabs in the upper mantle: insights from numerical and laboratory experiments. *J. Geophys. Res.* 104, 15207–15226.
- Becker, T.W., O'Connell, R.J., 2001. Predicting plate velocities with mantle circulation models. *Geochem. Geophys. Geosyst.*, 2.
- Bercovici, D., 1998. Generation of plate tectonics from lithosphere-mantle flow and void-volatile self-lubrication. *Earth Planet. Sci. Lett.* 154, 139–151.
- Bercovici, D., Ricard, Y., Richards, M.A., 2000. The relation between mantle dynamics and plate tectonics: a primer. *Geophys. Monogr. Am. Geophys. Union* 121, 5–46.
- Biggin, A.J., Steinberger, B., Aubert, J., Suttie, N., Holme, R., Torsvik, T.H., van der Meer, D.G., van Hinsbergen, D.J.J., 2012. Possible links between long-term geomagnetic variations and whole-mantle convection processes. *Nat. Geosci.* 5, 526–533.
- Bird, P., 2003. An updated digital model of plate boundaries. *Geochem. Geophys. Geosyst.* 4, 1027. <http://dx.doi.org/10.1029/2001GC000252>.
- Brandenburg, J., van Keken, P., 2007. Methods for thermochemical convection in Earth's mantle with force-balanced plates. *Geochem. Geophys. Geosyst.* 8, Q11004.
- Buffett, B.A., Gable, C.W., O'Connell, R.J., 1994. Linear stability of a layered fluid with mobile surface plates. *J. Geophys. Res.* 99, 19885–19900.
- Buffett, B.A., Heuret, A., 2011. Curvature of subducted lithosphere from earthquake locations in the Wadati-Benioff zone. *Geochem. Geophys. Geosyst.* 12, Q06010.
- Buffett, B.A., Rowley, D.B., 2006. Plate bending at subduction zones: consequences for the direction of plate motions. *Earth Planet. Sci. Lett.* 245, 359–364.
- Capitanio, F., Morra, G., Goes, S., 2009a. Dynamics of plate bending at the trench and slab-plate coupling. *Geochem. Geophys. Geosyst.* 10, Q04002.
- Capitanio, F.A., Morra, G., Goes, S., 2007. Dynamic models of downgoing plate-buoyancy driven subduction: subduction motions and energy dissipation. *Earth Planet. Sci. Lett.* 262, 284–297.
- Capitanio, F.A., Morra, G., Goes, S., 2009b. Dynamics of plate bending at the trench and slab-plate coupling. *Geochem. Geophys. Geosyst.*, 10.
- Christensen, U., 2001. Geodynamic models of deep subduction. *Phys. Earth Planet. Inter.* 127, 25–34.
- Christensen, U.R., Yuen, D.A., 1984. The interaction of a subducting lithospheric slab with a chemical or phase boundary. *J. Geophys. Res.* 89, 4389–4402.
- Coltice, N., Rolf, T., Tackley, P., Labrosse, S., 2012. Dynamic causes of the relation between area and age of the ocean floor. *Science* 336, 335–338.
- Conrad, C. P., and M. D. Behn (2010), Constraints on lithosphere net rotation and asthenospheric viscosity from global mantle flow models and seismic anisotropy, *Geochem. Geophys. Geosyst.*, 11, Q05W05, <http://dx.doi.org/10.1029/2009GC002970>.
- Conrad, C.P., Hager, B.H., 1999. Effects of plate bending and fault strength at subduction zones on plate dynamics. *J. Geophys. Res.* 104, 17551–17571.
- Conrad, C.P., Lithgow-Bertelloni, C., 2002. How mantle slabs drive plate tectonics. *Science* 298, 207–209.
- Cramer, F., Tackley, P., Meilick, I., Gerya, T., Kaus, B., 2012. A free plate surface and weak oceanic crust produce single-sided subduction on Earth. *Geophys. Res. Lett.* 39, L03306.
- Creveling, J.R., Mitrovica, J.X., Chan, N.H., Latychev, K., Matsuyama, I., 2012. Mechanisms for oscillatory true polar wander. *Nature* 491, 244–248.
- Deschamps, F., Cobden, L., Tackley, P.J., 2012. The primitive nature of large low shear-wave velocity provinces. *Earth Planet. Sci. Lett.* 349, 198–208.
- Dziewonski, A.M., Lekic, V., Romanowicz, B.A., 2010. Mantle anchor structure: an argument for bottom up tectonics. *Earth Planet. Sci. Lett.* 299, 69–79.
- Faccenna, C., Davy, P., Brun, J.P., Funicello, R., Giardini, D., Mattei, M., Nalpas, T., 1996. The dynamic of backarc basins: an experimental approach to the opening of the Tyrrhenian Sea. *Geophys. J. Int.* 126, 781–795.
- Forsyth, D., Uyeda, S., 1975. On the relative importance of the driving forces of plate motion. *Geophys. J. R. Astron. Soc.* 43, 163–200.
- Fukao, Y., Obayashi, M., Nakakuki, T., 2009. Stagnant slab: a review. *Annu. Rev. Earth Planet. Sci.* 37, 19–46.
- Gerya, T., 2010. Dynamical instability produces transform faults at mid-ocean ridges. *Science* 329, 1047–1050.
- Goes, S., Capitanio, F.A., Morra, G., 2008. Evidence of lower-mantle slab penetration phases in plate motions. *Nature* 451, 981–984.
- Grigné, C., Labrosse, S., Tackley, P.J., 2007. Convection under a lid of finite conductivity in wide aspect ratio models: effect of continents on the wavelength of mantle flow. *J. Geophys. Res. B: Solid Earth*, 112.
- Gurnis, M., 1988. Large-scale mantle convection and the aggregation and dispersal of supercontinents. *Nature* 332, 695–699.
- Gurnis, M., Turner, M., Zahirovic, S., DiCaprio, L., Spasojevic, S., Müller, R.D., Boyden, J., Seton, M., Manea, V.C., Bower, D.J., 2012. Plate tectonic reconstructions with continuously closing plates. *Comput. Geosci.* 38, 35–42.
- Hirth, G., Kohlstedt, D.L., 1996. Water in the oceanic upper mantle: implications for rheology, melt extraction and the evolution of the lithosphere. *Earth Planet. Sci. Lett.* 144, 93–108.
- Husson, L., 2012. The dynamics of plate boundaries over a convecting mantle. *Phys. Earth Planet. Inter.* 212, 32–43.
- Husson, L., Conrad, C.P., Faccenna, C., 2012. Plate motions, Andean orogeny, and volcanism above the South Atlantic convection cell. *Earth Planet. Sci. Lett.* 317, 126–135.
- Iaffaldano, G., Bodin, T., Sambridge, M., 2012. Reconstructing plate-motion changes in the presence of finite-rotations noise. *Nat. Commun.* 3, 1048.
- Iaffaldano, G., Bunge, H.-P., Dixon, T.H., 2006. Feedback between mountain belt growth and plate convergence. *Geology* 34, 893–896.
- King, S.D., 2001. Subduction zones: observations and geodynamic models. *Phys. Earth Planet. Inter.* 127, 9–24.
- King, S.D., Lowman, J.P., Gable, C.W., 2002. Episodic tectonic plate reorganisations driven by mantle convection. *Earth Planet. Sci. Lett.* 203, 83–91.

- Lee, C., King, S.D., 2011. Dynamic buckling of subducting slabs reconciles geological and geophysical observations. *Earth Planet. Sci. Lett.* 312, 360–370.
- Lemery, C., Ricard, Y., Sommeria, J., 2000. A model for the emergence of thermal plumes in Rayleigh–Bénard convection at infinite Prandtl number. *J. Fluid Mech.* 414, 225–250.
- Li, Z.H., Ribe, N.M., 2012. Dynamics of free subduction from 3-D boundary element modeling. *J. Geophys. Res.: Solid Earth* 1978–2012, 117.
- Lithgow-Bertelloni, C., Gynn, J.H., 2004. Origin of the lithospheric stress field. *J. Geophys. Res.* 109, B01408.
- Lithgow-Bertelloni, C., Richards, M., 1998. The dynamics of Cenozoic and Mesozoic plate motions. *Rev. Geophys.* 36, 27–78.
- Lowman, J.P., 2011. Mantle convection models featuring plate tectonic behavior: an overview of methods and progress. *Tectonophysics* 510, 1–16.
- Lowman, J.P., King, S.D., Gable, C.W., 2001. The influence of tectonic plates on mantle convection patterns, temperature and heat flow. *Geophys. J. Int.* 146, 619–636.
- Lowman, J.P., King, S.D., Gable, C.W., 2003. The role of the heating mode of the mantle in intermittent reorganisation of the plate velocity field. *Geophys. J. Int.* 152, 455–467.
- Matthews, K.J., Seton, M., Müller, R.D., 2012. A global-scale plate reorganisation event at 105–100 Ma. *Earth Planet. Sci. Lett.* 355, 283–298.
- Miall, A.D., 1990. *Principles of Sedimentary Basins*. Springer-Verlag, New York.
- Monnereau, M., Quéré, S., 2001. Spherical shell models of mantle convection with tectonic plates. *Earth Planet. Sci. Lett.* 184, 575–587.
- Moresi, L., Dufour, F., Mühlhaus, H., 2002. Mantle convection models with viscoelastic-brittle lithosphere: numerical methodology and plate tectonic modeling. *Pure Appl. Geophys.* 159, 2335.
- Morra, G., L. Quevedo, and R. D. Müller (2012), Spherical dynamic models of top-down tectonics, *Geochim. Geophys. Geosyst.*, 13, Q03005, <http://dx.doi.org/10.1029/2011GC003843>
- Morra, G., Yuen, D., Boschi, L., Chatelain, P., Koumoutsakos, P., Tackley, P., 2010. The fate of the slabs interacting with a density/viscosity hill in the mid-mantle. *Phys. Earth Planet. Inter.* 180, 271–282.
- O'Farrell, K.A., Lowman, J.P., Bunge, H.P., 2013. Comparison of spherical-shell and plane-layer mantle convection thermal structure in viscously stratified models with mixed-mode heating: implications for the incorporation of temperature-dependent parameters. *Geophys. J. Int.* 192, 456–472.
- O'Neill, C., Lenardic, A., Griffin, W., O'Reilly, S.Y., 2008. Dynamics of cratons in an evolving mantle. *Lithos* 102, 12–24.
- O'Neill, C., Lenardic, A., Jellinek, A., Moresi, L., 2009. Influence of supercontinents on deep mantle flow. *Gondwana Res.* 15, 276–287.
- Olson, P.L., Coe, R.S., Driscoll, P.E., Glatzmaier, G.A., Roberts, P.H., 2010. Geodynamo reversal frequency and heterogeneous core–mantle boundary heat flow. *Phys. Earth Planet. Inter.* 180, 66–79.
- Phillips, B.R., Coltice, N., 2010. Temperature beneath continents as a function of continental cover and convective wavelength. *J. Geophys. Res.* 115, B04408.
- Regenauer-Lieb, K., Hobbs, B., Yuen, D.A., Ord, A., Zhang, Y., Mühlhaus, H.B., Morra, G., 2006. From point defects to plate tectonic faults. *Philos. Mag.* 86, 3373–3392.
- Regenauer-Lieb, K., Yuen, D., Branlund, J., 2001. The initiation of subduction: criticality by addition of water? *Science* 294, 578–580.
- Ribe, N.M., 2010. Bending mechanics and mode selection in free subduction: a thin-sheet analysis. *Geophys. J. Int.* 180, 559–576.
- Ricard, Y., 2007. Physics of mantle convection. *Treatise Geophys.* 7, 31–87.
- Ricard, Y., Vigny, C., 1989. Mantle dynamics with induced plate tectonics. *J. Geophys. Res.* 94, 17543–17559.
- Richards, M.A., Engebretson, D.C., 1992. Large-scale mantle convection and the history of subduction. *Nature* 355, 437–440.
- Rolf, T., Coltice, N., Tackley, P., 2012. Linking continental drift, plate tectonics and the thermal state of the Earth's mantle. *Earth Planet. Sci. Lett.* 351, 134–146.
- Schuberth, B., Bunge, H.P., Steinle-Neumann, G., Moder, C., Oeser, J., 2009. Thermal versus elastic heterogeneity in high-resolution mantle circulation models with pyrolytic composition: high plume excess temperatures in the lowermost mantle. *Geochim. Geophys. Geosyst.*, 10.
- Scriven, L.E., Sternling, C.V., 1964. On cellular convection driven by surface-tension gradients: effects of mean surface tension and surface viscosity. *J. Fluid Mech. Digital Arch.* 19, 321–340.
- Seton, M., Müller, R.D., Zahirovic, S., Gaina, C., Torsvik, T., Shephard, G., Talsma, A., Gurnis, M., Turner, M., Maus, S., Chandler, M., 2012b. Global continental and ocean basin reconstructions since 200 Ma. *Earth Sci. Rev.* 113, 212–270.
- Skarda, J.R.L., McCaughan, F.E., 1994. Coupled Marangoni–Benard/Rayleigh–Benard Instability with Temperature Dependent Viscosity. NASA STI/Recon Technical Report no. 94, 37507.
- Sornette, D., Pisarenko, V., 2003. Fractal plate tectonics. *Geophys. Res. Lett.* 30 1105.
- Stegman, D.R., Schellart, W.P., Freeman, J., 2010. Competing influences of plate width and far-field boundary conditions on trench migration and morphology of subducted slabs in the upper mantle. *Tectonophysics* 483, 46–57.
- C. Stein, J.P. Lowman, U. Hansen, The influence of mantle internal heating on lithospheric mobility: Implications for super-Earths, *Earth and Planetary Science Letters*, Volume 361, 1 January 2013, Pages 448–459, ISSN 0012–821X, <http://dx.doi.org/10.1016/j.epsl.2012.11.011>.
- Steinberger, B., Torsvik, T.H., 2008. Absolute plate motions and true polar wander in the absence of hotspot tracks. *Nature* 452, 620–623.
- Steinberger, B., Torsvik, T.H., 2010. Toward an explanation for the present and past locations of the poles. *Geochim. Geophys. Geosyst.* 11, Q06W06.
- Tackley, P., 2000. Self-consistent generation of tectonic plates in time- dependent, three-dimensional mantle convection simulations, 1. Pseudoplastic yielding. *Geochim. Geophys. Geosyst.*, 01.
- Thess, A., Spirn, D., Juttner, B., 1997. A two-dimensional model for slow convection at infinite Marangoni number. *J. Fluid Mech.* 331, 283–312.
- Torsvik, T.H., Müller, R.D., Van der Voo, R., Steinberger, B., Gaina, C., 2008a. Global plate motion frames: toward a unified model. *Rev. Geophys.* 46, RG3004.
- Torsvik, T.H., Steinberger, B., Cocks, L.R.M., Burke, K., 2008b. Longitude: linking Earth's ancient surface to its deep interior. *Earth Planet. Sci. Lett.* 276, 273–282.
- Trompert, R., Hansen, U., 1998. Mantle convection simulations with rheologies that generate plate-like behaviour. *Nature* 395, 686–689.
- van der Hilst, R.D., Káráson, H., 1999. Compositional heterogeneity in the bottom 1000 km of Earth's mantle: toward a hybrid convection model. *Science* 283, 1885–1888.
- van der Meer, D.G., Spakman, W., van Hinsbergen, D.J.J., Amaru, M.L., Torsvik, T.H., 2009. Towards absolute plate motions constrained by lower-mantle slab remnants. *Nat. Geosci.* 3, 36–40.
- van Keken, P.E., Ballentine, C.J., 1998. Whole-mantle versus layered mantle convection and the role of a high-viscosity lower mantle in terrestrial volatile evolution. *Earth Planet. Sci. Lett.* 156, 19–32.
- Veevers, J.J., 2000. Change of tectono-stratigraphic regime in the Australian plate during the 99 Ma (mid-Cretaceous) and 43 Ma (mid-Eocene) swerves of the Pacific. *Geology* 28, 47–50.
- Watts, A.B., Zhong, S., 2000. Observation of flexure and the rheology of oceanic lithosphere. *Geophys. J. Int.* 142, 855–875.
- Wessel, P., Harada, Y., Kroenke, L.W., 2006. Toward a self-consistent, high-resolution absolute plate motion model for the Pacific. *Geochim. Geophys. Geosyst.*, 7.
- Whittaker, J., Müller, R.D., Leitchkov, G., Stagg, H., Sdrolias, M., Gaina, C., Goncharov, A., 2007. Major Australian–Antarctic plate reorganisation at Hawaiian–Emperor bend time. *Science* 318, 83–86.
- Wuming, B., Vigny, C., Ricard, Y., Froidevaux, C., 1992. On the origin of deviatoric stresses in the lithosphere. *J. Geophys. Res.* 97, 11729–11737.
- Yanagisawa, T., Yamagishi, Y., 2005. Rayleigh–Benard convection in spherical shell with infinite Prandtl number at high Rayleigh number. *J. Earth Simulator* 4, 11–17.
- Yoshida, M., 2010. Preliminary three-dimensional model of mantle convection with deformable, mobile continental lithosphere. *Earth Planet. Sci. Lett.* 295, 205–218.
- Zhang, N., Zhong, S., McNamara, A.K., 2009. Supercontinent formation from stochastic collision and mantle convection models. *Gondwana Res.* 15, 267–275.
- Zhong, S., Gurnis, M., 1995. Mantle convection with plates and mobile, faulted plate margins. *Science* 267, 838–842.
- Zhong, S., McNamara, A., Tan, E., Moresi, L., Gurnis, M., 2008. A benchmark study on mantle convection in a 3-D spherical shell using CitcomS. *Geochim. Geophys. Geosyst.* 9, Q10017.
- Zhong, S., Zhang, N., Li, Z.-X., Roberts, J.H., 2007. Supercontinent cycles, true polar wander, and very long-wavelength mantle convection. *Earth Planet. Sci. Lett.* 261, 551–564.
- Zhong, S., Zuber, M.T., Moresi, L., Gurnis, M., 2000. Role of temperature-dependent viscosity and surface plates in spherical shell models of mantle convection. *J. Geophys. Res.* 105, 11063–11082.